scientific reports

Check for updates

OPEN

Radiogenomic analysis of clinical and ultrasonic characteristics in correlation to immune-related genes in breast cancer

Tingyao Dou[1,7], Yaodong Chen[2,7]✉, Lunhang Liu[1,7], Yaochen Zhang[1], Wanru Pei[1], Jing Li[3], Yan Lei[3], Yanhong Wang[4,5,6]✉ & Hongyan Jia[3,5]✉

Breast ultrasound plays a significant role in the non-invasive screening and diagnosis of breast cancer. The application of immunotherapy for breast cancer can significantly prolong the overall survival of advanced patients, which is an important research area of breast cancer treatment. The combination of ultrasound and immunotherapy helps patients diagnose and predict survival and develop a personalized treatment plan. This study analyzed the correlation between the clinical and ultrasonic characteristics of breast cancer and immune-related genes. First, the differential expression of immune-related genes was obtained using the GEO and IMMPORT database. Then, differentially expressed immune-related genes related to the overall survival of breast cancer were obtained using the GEPIA and Kaplan-Meier plotter platforms. Additionally, clinical, ultrasonic characteristics and pathological specimens of breast cancer patients' tumors were collected. Whole transcriptome sequencing and immunohistochemical staining were performed on the tumor specimens to obtain gene expression. CXCL2, MIA, NR3C2, PTX3, S100B, SAA1, SAA2, and CXCL9 genes were correlated with each other and with clinical and ultrasonic characteristics. The high expression of MIA was related to the positive expression of PR in breast cancer. The low expression of NR3C2 was correlated with the clinical characteristics of tumor size ≥ 20 mm, later stage, Her-2 positive, Ki-67 ≥ 20%. NR3C2 was negatively correlated with the value of PKI and AUC in contrast-enhanced ultrasound parameters, and positively correlated with the value of AT and TTP. The expression of the PTX3 gene was also negatively correlated with the value of PKI and Emax of shear wave elastography. SAA2 was related to the presence or absence of edge burrs characterized by ultrasound. The expression of the CXCL9 gene was associated with the age of onset and tumor stage. In this study, 8 differentially expressed immune-related genes related to the overall survival of breast cancer were screened, which had been proved to be associated with some characteristics of cancer in previous studies, and could be further studied in the subsequent immunotherapy of breast cancer. Some clinical and ultrasonic characteristics of breast cancer were significantly correlated with immune-related genes, such as NR3C2, SAA2, and CXCL9. Further analysis of these genes provides new ideas for the diagnosis and treatment of breast cancer.

Keywords Breast cancer, Breast ultrasound, Immune gene, Radiogenomics, Immunotherapy targets

According to the American Cancer Society, breast cancer is still the highest incidence of cancer among women in the world in 2024, accounting for 32% of the total incidence of female cancer. Still, the mortality rate of breast cancer only accounts for 15% of all cancers, ranking second[1]. Breast cancer treatment includes not only traditional surgical resection, radiotherapy, and chemotherapy, but also endocrine therapy, targeted therapy, and immunotherapy, which bring hope to breast cancer patients[2,3]. Thanks to the variety of treatments for breast

[1]Department of First Clinical Medicine, Shanxi Medical University, Taiyuan, Shanxi, China. [2]Department of Ultrasonic Imaging, First Hospital of Shanxi Medical University, Taiyuan 030001, Shanxi, China. [3]Department of Breast Surgery, First Hospital of Shanxi Medical University, Taiyuan, Shanxi, China. [4]Department of Microbiology and Immunology, School of Basic Medical Sciences, ShanxiMedical University, Taiyuan, Shanxi, China. [5]key Laboratory of Cellular Physiology, Shanxi Medical University, Ministry of Education, Taiyuan, Shanxi, China. [6]Department of Microbiology and Immunology, Shanxi Medical University, Taiyuan, Shanxi, China. [7]Tingyao Dou, Yaodong and Lunhang Liu contributed equally to this work. ✉email: chenyaodong@sxmu.edu.cn; wangyanhongmail@126.com; swallow_jhy@163.com

cancer, the 5-year survival rate for breast cancer is improving year by year[1]. It is well known that the survival of patients with early breast cancer is much better than that of advanced breast cancer. Therefore, breast cancer screening for all women can increase the early detection rate and diagnosis rate of breast cancer to reduce the mortality rate of breast cancer.

In China, the most routine examination of the breast is breast ultrasound. By using advanced and clear two-dimensional ultrasound equipment, experienced ultrasound doctors can observe the presence or absence of breast hyperplasia, mammary duct dilatation, and breast nodules[4]. Ultrasound can accurately detect small nodules that doctors cannot accurately examine. The possibility of malignant breast nodules is judged by whether the shape of the nodules is regular, whether the aspect ratio is greater than 1, whether the posterior echo is attenuated, whether there is a rich blood flow signal, echo pattern, and so on. Ultrasound can also be used in surgery, such as ultrasound-guided percutaneous A1 pulley release[5] and mammotome-assisted surgery for patients with breast benign tumors[6]. Now, more advanced breast ultrasound instruments are being developed, such as Mindray Nuewa R9 Pro ultrasound diagnostic instrument, which can accurately detect the micro blood flow of breast nodules (including blood flow index, perforator vessels, etc.) and hardness, which is more helpful for ultrasound doctors to judge the nature of breast nodules. At present, studies have been made to use various ultrasonic characteristics of breast nodules to predict molecular type, stage, gene expression, and even tissue hypoxia in breast cancer[7–9]. Therefore, some ultrasonic characteristics have good predictive value for breast cancer, but more in-depth research still needs to be widely studied in clinics in the future.

Radiogenomics is a new research field, which studies the relationship between tumor imaging characteristics and genomic characteristics. Radiogenomics of tumors can non-invasively reveal potential biological functional characteristics related to imaging characteristics and reveal potential carcinogenic mechanisms. It improves the accuracy of patient treatment by improving non-invasive prediction and survival prediction at the molecular level of the tumor[10]. At present, the use of radiogenomics to explore the diagnosis and treatment of breast cancer has been widely studied[11]. However, multiple radiogenomics studies use the parameters of breast nuclear magnetic resonance (NMR)[12,13], and only a few studies use the characteristics of breast ultrasound. In addition, compared with European and American women, Chinese women's breasts are smaller in size, with an average thickness of 3.5 cm and a denser density, so ultrasound examination is more suitable and accurate. Therefore, we believe that ultrasound imaging characteristics have more advantages than NMR characteristics, and its application in breast cancer radiogenomics is novel and prospective, and ultrasound examination has the advantages of non-invasiveness, low price, and short examination time.

So far, the treatment of breast cancer has come to the era of precision therapy. The emergence and clinical application of immunotherapy such as PD-1/PD-L1 and CTLA-4 inhibitors[14] have benefited many cancer patients and brought hope to breast cancer immunotherapy. The mechanism of immunotherapy is to enhance the anti-tumor activity of $CD8^{+}$T cells by presenting tumor-associated antigens to T lymphocytes through dendritic cells in patients, thereby inhibiting the development of breast cancer[15]. TIM-3, TIGIT, and VISTA are relatively clear immune-related genes in breast cancer patients[16–18], but their therapeutic effects are unclear.

In this study, we explored the correlation between clinical and ultrasonic characteristics of breast cancer and immune-related genes (Fig. 1). Firstly, the Gene Expression Omnibus (GEO) database was used to screen the differentially expressed genes (DEGs) in breast cancer and adjacent normal tissues. Then the immune-related genes (IRGs) in the IMMPORT database were used to intersect the two to obtain the differentially expressed immune-related genes (DEIRGs). The Gene Expression Profiling Interactive Analysis (GEPIA) and Kaplan-Meier (KM) plotter platforms were used to screen the DEIRGs related to the overall survival of breast cancer. The clinical and ultrasonic characteristics of breast cancer patients were collected. Pathological specimens obtained from the pathology department, First Hospital of Shanxi Medical University, were subjected to whole transcriptome sequencing and immunohistochemical staining. The expression of the screened genes was extracted from the whole transcriptome sequencing database, and the clinical characteristics and ultrasonic characteristics of the patients were statistically analyzed. The conclusion of this study was to screen for DEIRGs related to the overall survival of breast cancer, which can be further studied in breast cancer immunotherapy. Some ultrasonic and clinical characteristics of breast cancer were significantly correlated with immune-related genes. Further analysis provides new ideas for the diagnosis and treatment of breast cancer.

Methods

Patients

Inclusion criteria: (1) Breast patients admitted to the First Hospital of Shanxi Medical University from January 2023 to December 2023 who completed breast B-mode ultrasound, microvascular imaging, strain shear wave elastography (SWE), and contrast-enhanced ultrasound (CEU), and saved ultrasound image data, (2) postoperative paraffin pathology showed malignant breast tumors, (3) patients who have no chronic disease, or whose chronic disease has been well controlled. Exclusion criteria: (1) patients with incomplete clinical and pathological data, (2) patients who have undergone breast cancer-related treatment (including breast puncture, surgery, chemotherapy, radiation, and endocrine therapy), (3) patients with other malignant tumors or serious diseases, (4) patients whose remaining tumor tissue in the pathology department is too little to perform whole transcriptome sequencing. This retrospective study passed the ethical review and the patient's informed consent for the use of the specimens has been exempted.

Data analysis screened differentially expressed immune-related genes

GEO database contains a large number of published gene expression data sets in various countries around the world, providing free open download and application for the public[19]. Using 'breast cancer' and 'Homo sapiens' as key words, microarray data were searched for in the GEO database. The final selected breast cancer gene

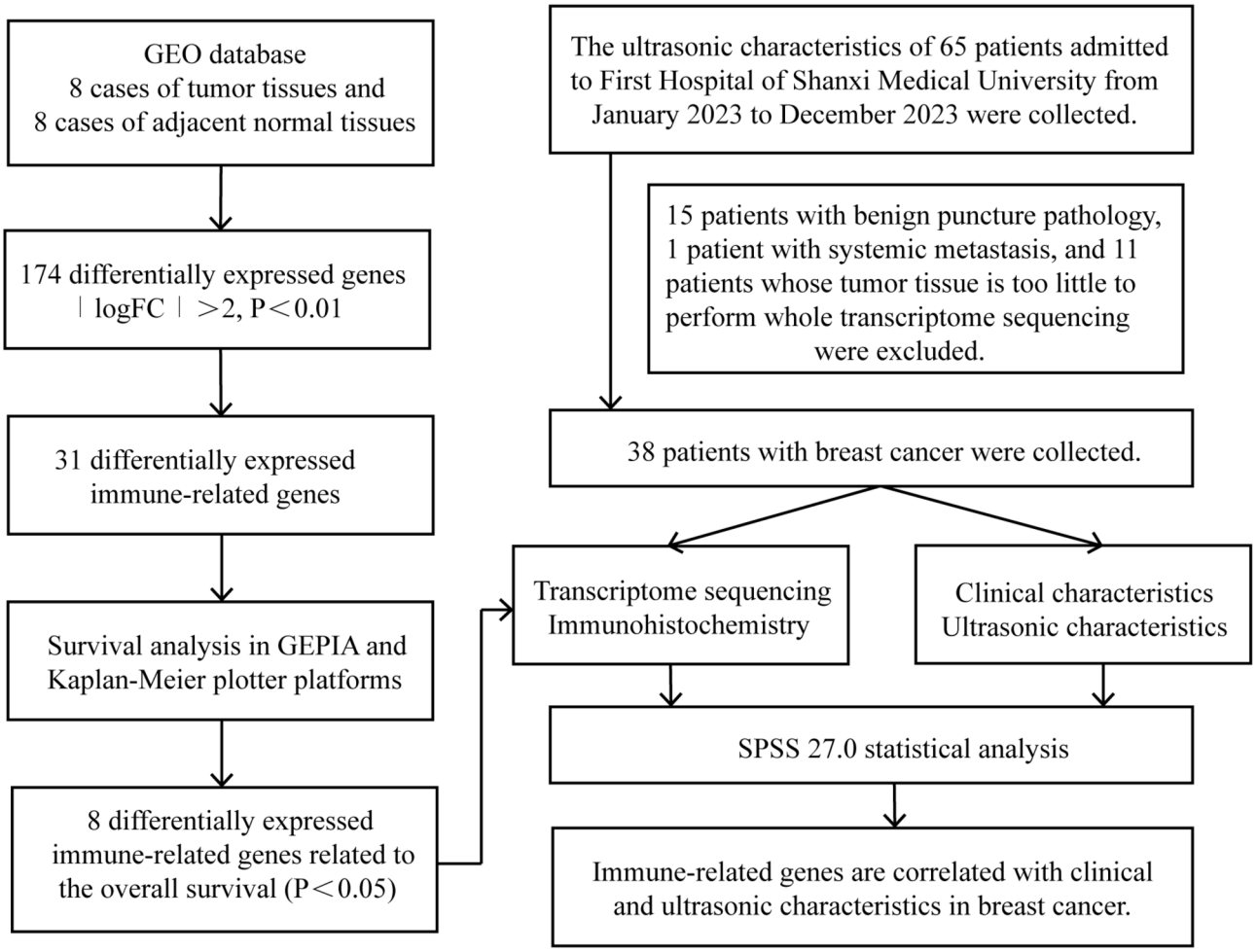

Fig. 1. Schematic of research strategy.

expression dataset GSE33447 consists of 8 tumor tissues and 8 adjacent normal tissues[20]. IMMPORT Shared Data is an authoritative database of immunology, providing immunological data and analysis tools that can be used to query immune genes[21]. The list of immunology-related genes on this site has been compiled from the Reactome database of "Immune System" events and the GO database of "Immune System Process" terms. We have downloaded the full list of immune-related genes from IMMPORT (version 2023)[22]. The DEGs between breast cancer and adjacent normal tissues were determined by R package "limma" (version 3.58.1). The raw data were background corrected using the backgroundCorrect function, averaged over multiple probes for the same gene using the avereps function to ensure that only unique expression values were retained for each gene, and normalized to the original data by quartile normalization using the normalizeBetweenArrays function. NormaliseBetweenArrays is a function that normalizes raw data. To test for potential internal batch effects, we created box plots of each sample's distribution.

Genes with a |logFC|> 2 and a $p<0.01$ were defined as DEGs. The R package "dplyr" was used to find differentially expressed genes with immune-related genes. DEIRGs were obtained by merging the previously acquired DEGs list with the immune gene data in the IMMPORT database, followed by Venn diagram analysis to visualize overlapping candidates.

GEPIA and Kaplan-Meier plotter platforms analysis

GEPIA is a web server for cancer and normal gene expression analysis and interaction analysis. GEPIA collates the expression values of each searchable gene in different tumor samples. It can calculate the expression level of a gene in a certain tumor, analyze the relationship between genes and tumor prognosis, and co-expression between genes[23]. The KM survival curve contains gene expression data and survival information of breast cancer patients. The survival information on KM includes OS, RFS, DMFS, and PPS of cancer patients. It is a powerful tool for analyzing patient survival outcomes[24]. We obtained the relationship between the DEIRGs and the overall survival of breast cancer patients through GEPIA and KM, and further screened the DEIRGs that affect the survival and prognosis of breast cancer patients.

Ultrasonic characteristics

In this study, Mindray Nuewa R9 Pro ultrasonic diagnostic instrument (Mindray Medical, China) equipped with L15-3WU ultrasonic probe was used to collect and store ultrasonic data, including B-mode ultrasound, microvascular imaging, SWE, and CEU. B-mode ultrasonic characteristics are qualitative analysis, including aspect ratio (> 1 and ≤ 1), with or without edge burrs, and calcification. Microvascular imaging characteristics, SWE characteristics, and contrast-enhanced ultrasonic characteristics (CEUS) belong to quantitative analysis. Microvascular imaging characteristics include color Doppler flow imaging (CDFI) and ultramicro angiography (UMA). Microvascular imaging can display blood flow direction, blood flow velocity, and blood flow dispersion. The faster the blood flow velocity, the higher the sensitivity of the blood flow pixel ratio. The characteristics of CDFI and UMA include: using the built-in analysis software of the ultrasonic diagnostic instrument, manually outlining the boundary of the lesion as the region of interest (ROI), and obtaining the color pixel percentage (CPP) of the lesion, hereinafter referred to as CDFI-CPP and UMA-CPP. The characteristics of SWE include Young's modulus E_{mean}, E_{max}, E_{min}, and E_{sd}[25]. The E_{mean} value reflects the average Young's modulus of the whole area of the breast mass; the E_{max} value reflects the Young's modulus value of the hardest part of the breast mass; the E_{min} value is the minimum value of Young's modulus of SWE. E_{sd} value reflects the degree of variation of Young's modulus in different regions of breast mass. CEUS include peak intensity (PKI), area under the curve (AUC), contrast agent development time (AT), and time to peak (TTP), which are used to indicate the blood supply of local lesions[26]. Important ultrasonic diagnostic instrument parameters: (1) ultrasonic probe frequency is 15 MHz, (2) image depth is 4 cm, (3) B-mode ultrasound gain is 38, (4) CDFI gain is 52, scale is -3.3 ~ 3.3, (5) UMA gain is 34, scale is -2.1 ~ 2.1, (6) CEUS gain is 55. Image analysis was performed by two sonographers with more than 5 years of experience in ultrasound diagnosis, and in case of disagreement, the decision was made in consultation with another sonographer with more than 10 years of experience in breast tumor diagnosis to maintain the reliability of the results and the consistency of the testing standards.

Whole transcriptome sequencing

In order to analyze the expression of DEIRGs related to breast cancer overall survival, whole transcriptome sequencing was performed on tumor tissues of 38 patients with breast cancer. Following the manufacturer's instructions, TRIzol® Reagent was used to extract total RNA. The quality of RNA was assessed using the 5300 Bioanalyser (Agilent) and quantified with the ND-2000 (NanoDrop Technologies). Only RNA samples meeting high-quality criteria (OD260/280 = 1.8 ~ 2.2, OD260/230 ≥ 2.0, RQN ≥ 6.5, 28 S:18 S ≥ 1.0, and > 1 μg) were utilized for sequencing library construction. RNA Purification Kit was used to purify nucleic acid. The kit used in this experiment used Illumina® Stranded Total RNA Prep, Ligation with Ribo-Zero Plus, and Microbiome for library preparation. They were sequenced by using the NovaSeq Reagent Kit.

Immunohistochemical staining

Immunohistochemical staining was performed on the paraffin sections of the selected genes with high expression in breast cancer to analyze the DEIRGs related to the overall survival of breast cancer. The pathological sections used for immunohistochemical analysis were all from First Hospital of Shanxi Medical University. Breast cancer patients included in this study were screened again, and patients who underwent neoadjuvant therapy and did not undergo surgical treatment were excluded. Immunohistochemical staining was performed on 22 cases of breast cancer and adjacent tissues. 5 cases of renal cell carcinoma were stained as the positive control for the immunohistochemical process before the formal experiment. Firstly, paraffin-embedded slides were dewaxed and rehydrated with xylene and graded series of ethanol (100%, 95%, 80%, 75%). Then the citrate repair solution was boiled at the high temperature (180℃) in a pressure cooker for 2 min and cooled under flowing water to repair the antigen on the slice. Then the peroxidase blocker was added dropwise at room temperature in the dark for 15 min. Then incubated with anti-CXCL9 (Wuhan Sanying Biotechnology Co., LTD) primary antibody (1:100) in a wet chamber at 37 °C for 1.5 h. The slides were incubated with the secondary antibody (Beijing Zhongshan Jinqiao Biotechnology Co., LTD) for 30 min at room temperature. Washed with PBS 3 times between each step, 5 min each time. For the color reaction, the slide was incubated with the DAB solution. Subsequently, the slides were counter-stained with hematoxylin, dehydrated with graded alcohol series, and covered with neutral balsam. The immunohistochemical results were quantified by a combination of ImageJ and microscopic counting. The microscopic counting was independently read by 2 pathologists with more than 5 years of clinical experience in the First Hospital of Shanxi Medical University, and the relevant data were set blind. The brown-colored positive cells on the tissue slides in 3 fields were randomly selected under a 400x microscope, and the average of the positive cells in 3 fields was counted. The number of positive cells was quantified as immunohistochemical results.

Statistical analysis

R (version 4.2.1) was used to process the data of GEO and IMMPORT database and make heat maps, volcano maps, and Wayne maps. SPSS 27.0 performed statistical analysis of the correlation between clinical characteristics, ultrasonic characteristics, and gene expression levels and created correlation scatter plots. The patient's age and tumor size were expressed as mean ± standard deviation (x ± s), and menopause, stage, and classification were expressed as number and percentage (%). SPSS was used to analyze whether the continuous data variables obeyed normal distribution, and all the continuous ultrasonic characteristics and gene expression data characteristics in our data obeyed non-normal distribution. Therefore, for the hypothesis test of classification characteristics (such as TNM stage, with or without edge burrs, calcification, etc.), non-parametric T-test was used for data characteristics. Two independent samples were tested by the Mann-Whitney U test, Kolmogorov-Smirnov, or Moses extreme reaction test according to different data characteristics. The Kruskal-Wallis test was used for

multiple independent samples. Spearman correlation analysis was used to test the hypothesis of continuous variables (such as gene expression and characteristic parameters of ultrasound), because none of our data obeys a normal distribution. Sanger Box biomedical big data analysis platform was used to analyze the correlation between differentially expressed genes[27,28]. The reliability and significance of the statistical results were assessed by confidence intervals (CI) and P values. $P<0.05$ was considered statistically significant.

Results

Clinical characteristics of patients

This study included 38 patients with breast cancer. The clinical characteristics of the patients (including age, menopausal status, tumor size, and molecular typing) are shown in Table 1. The average size of breast cancer is 23.42 mm (range 10.4 ~ 43.3 mm). These patients are female, and paraffin pathology results are invasive ductal carcinoma.

DEGs and IRGs in breast cancer

Gene expression data of 8 cases of breast cancer and 8 cases of adjacent normal tissues were downloaded from the GEO database. Quantile-normalized expression values exhibited tightly aligned distributions across all samples, as visualized in supplementary box plots (Figure S1), suggesting negligible intra-cohort batch effects. A total of 174 differentially expressed genes were screened out (Fig. 2a). 111 differentially expressed genes were lowly expressed in breast cancer, and 63 differentially expressed genes were highly expressed in breast cancer (Fig. 2b). Using the data in the IMMPORT database, 31 DEIRGs were screened (Fig. 2c). Among them, 20 genes were lowly expressed in breast cancer, and 11 genes were highly expressed. The specific name, modified P value, logFC, and up or down-regulation of 31 genes are listed in Table 2.

The expression of DEIRGs and their relationship with overall survival

The expression of these 31 genes and their correlation with overall survival were obtained in GEPIA and Kaplan-Meier plotter platforms. A total of 8 genes were associated with overall survival ($P<0.05$) in both database platforms (Table 2), namely CXCL2, MIA, NR3C2, PTX3, S100B, SAA1, SAA2 and CXCL9, of which 7 genes were lowly expressed and 1 gene was lowly expressed in breast cancer, which was consistent with previous results. The curves of these 8 genes in the two databases with the overall survival of patients are shown in Fig. 3a and b. The results showed that the overall survival of patients with high expression of these 8 genes was higher. The specific expression of these 8 immune-related genes in breast cancer was obtained in GEPIA (Fig. 3c) and

Clinical characteristics	Number	Frequency
Age(years)	52.82 ± 9.83	
≥ 60	23	60.53%
< 60	15	39.47%
Menopause		
Yes	20	52.6%
No	18	47.4%
Tumor size(mm)	23.42 ± 8.51	
< 20 mm	16	42.1%
≥ 20 mm	22	57.9%
Positive lymph nodes		
Yes	20	52.6%
No	18	47.4%
TNM Stage		
IA	10	26.3%
IIA	13	34.2%
IIB	15	39.5%
Immunohistochemical results		
LuminalA	7	18.4%
LuminalB	14	36.8%
Her-2 +(HR+)	7	18.4%
Her-2 +(HR-)	7	18.4%
Triple-Negative	3	7.9%
ER positive	28	73.7%
PR positive	23	60.5%
HER-2 positive	14	36.8%
Ki-67 ≥ 20%	26	68.4%

Table 1. Clinical characteristics of patients. Data are displayed as mean ± standard deviation (x ± s). ER estrogen receptor, PR progesterone receptor, HER-2 human epidermal growth factor receptor 2.

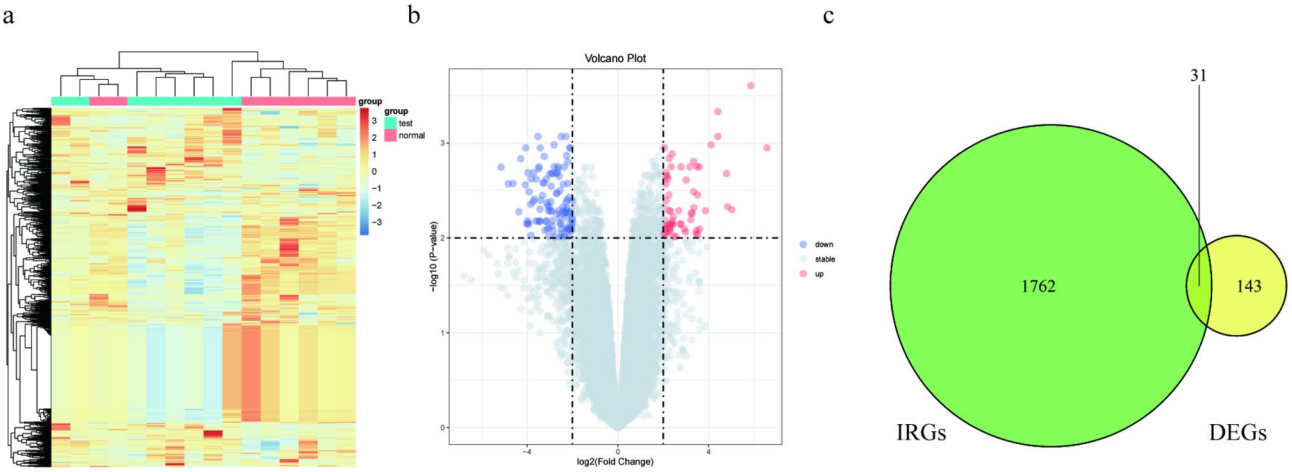

Fig. 2. Using GEO and IMMPORT databases to screen out DEIRGs in breast cancer. (**a**) Heatmap of differentially expressed genes. (**b**) Volcanic map of high and low expression of DEGs, in which the blue dot is a gene with low expression, and the red dot is a gene with high expression in breast cancer. (**c**) Wayne map of the intersection of differentially expressed genes and immune-related genes .

Gene	adj.*P*.Val	logFC	change	OS(logrank)GEPIA	OS(logrank)KM
BMP8A	0.008947	2.1	up	0.79	**0.0094**
CCL28	0.002098	-2.88	down	0.12	0.11
CCR8	0.007918	2.29	up	0.73	0.13
CD70	0.002701	2.12	up	0.16	0.21
CXCL10	0.003527	3.51	up	0.61	**0.0061**
CXCL11	0.008336	3.47	up	0.51	**0.042**
CXCL2	0.002391	-3.82	down	**0.0039**	**0.042**
CXCL9	0.005165	3.86	up	**0.0049**	**0.0011**
DEFB1	0.002404	-3.6	down	0.31	**0.00064**
DMBT1	0.00961	-2.14	down	0.22	**0.0086**
ESM1	0.008056	2.94	up	0.22	**0.0001**
FAM3D	0.008056	-3.09	down	0.053	**0.0049**
FGF2	0.008452	-2.23	down	0.24	0.0024
FOS	0.009983	-2.39	down	0.14	**0.000021**
IL21R	0.001299	2.39	up	0.96	**0.0005**
IL22RA1	0.006937	-2.02	down	0.053	**0.077**
LIFR	0.006145	-2.26	down	0.22	**0.00034**
MIA	0.006937	-3.94	down	**0.0014**	**0.0003**
MSR1	0.00178	2.35	up	0.37	**0.027**
NPPA	0.006557	-2.87	down	0.097	0.11
NR3C2	0.006422	-2.01	down	**0.027**	**0.036**
OLR1	0.005477	3.26	up	0.31	0.18
PENK	0.002763	-4.08	down	0.21	**0.0019**
PF4V1	0.005165	-2.61	down	Not found	0.11
PTN	0.001125	-3.42	down	0.1	0.19
PTX3	0.002854	-2.94	down	**0.037**	**0.026**
S100B	0.005223	-2.93	down	**0.031**	**0.0012**
SAA1	0.004015	-3.41	down	**0.0068**	**0.024**
SAA2	0.00178	-3.48	down	**0.048**	**0.0042**
TNFRSF9	0.00178	2.78	up	0.98	**0.000035**
TSLP	0.001353	-2.26	down	0.096	0.29

Table 2. DEIRGs in breast cancer and their correlation with overall survival. Significant values are in bold.

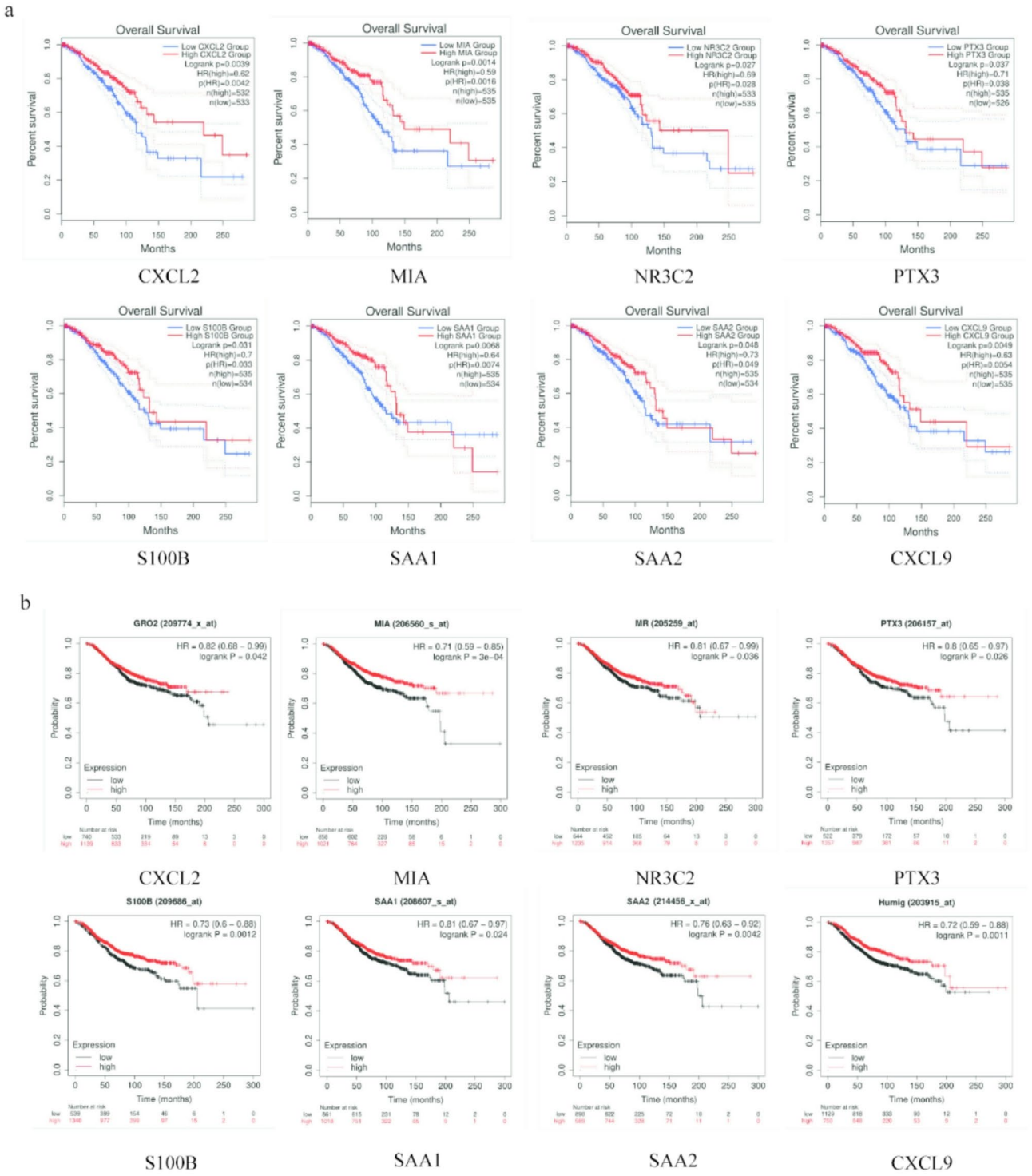

Fig. 3. Survival curve and expression of DEIRGs in public databases. (**a**) Overall survival in patients with high or low expression of DEIRGs in GEPIA. (**b**) Overall survival in patients with high or low expression of DEIRGs in Kaplan-Meier Plotter platforms. In the GEPIA database and Kaplan-Meier Plotter, breast cancer patients with high expression of CXCL2, MIA, NR3C2, PTX3, S100B, SAA1, SAA2, and CXCL9 genes had higher overall survival. (**c**) Scatter plot of gene expression in breast cancer and adjacent tissues in GEPIA. The expression of CXCL2, MIA, NR3C2, PTX3, S100B, SAA1 and SAA2 genes was low in breast cancer, while the expression of CXCL9 gene was high. (d) Violin plot of gene expression in different stages of breast cancer in GEPIA. The expression of CXCL2, S100B and SAA1 was negatively correlated with the stage of breast cancer.

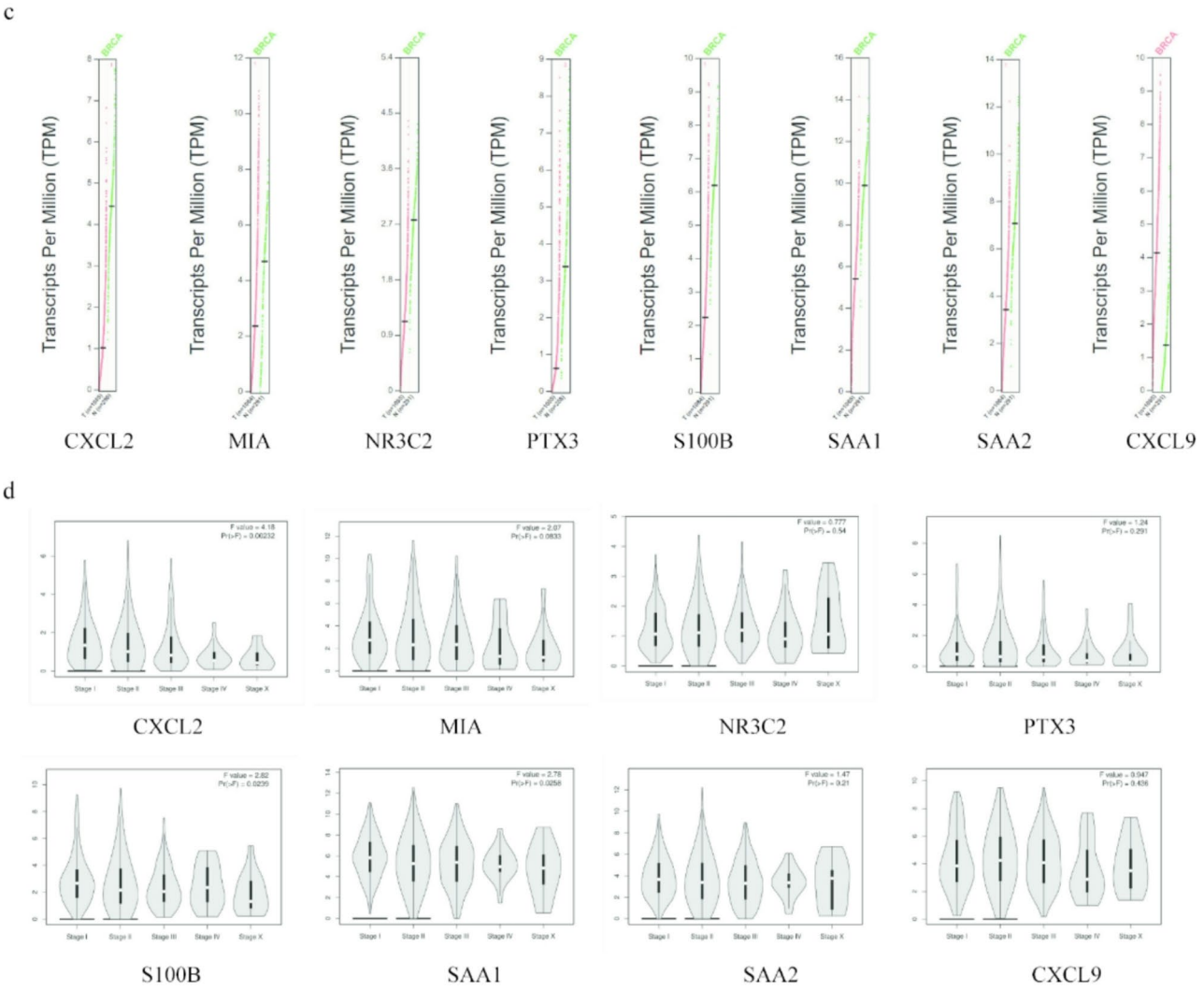

Figure 3. (continued)

the relationship between different breast cancer stages (Fig. 3d). The expression of CXCL2, S100B, and SAA1 in different stages of breast cancer was statistically different ($P<0.05$), and the later the stage of the tumor, the lower the expression of these genes. We extracted the expression of these 8 genes in the whole transcriptome sequencing database for subsequent analysis.

Correlation between DEIRGs and clinical characteristics of breast cancer

Table 3 shows the relationship between 8 immune-related genes and different clinical characteristics. The age-related genes were S100B and CXCL9. Low expression of S100B (median, 0.62vs0.72, $P=0.035$) and high expression of CXCL9 (median, 26.31vs4.59, $P=0.004$) were found in patients aged ≥ 60 years. The NR3C2 gene was associated with tumor size. Patients with tumor size ≥ 20 mm usually had low expression of NR3C2 (median, 0.95 vs. 2.63, $P=0.001$). The genes related to breast cancer TNM stage were NR3C2, S100B, and CXCL9. As the clinical stage of the patients became later, the expression of NR3C2 gradually decreased (median, 2.46vs1.97vs0.93, $P=0.034$), the expression of S100B increased first and then decreased (median, 0.76vs1.24vs0.52, $P=0.048$), and the expression of CXCL9 also increased first and then decreased (median, 5.55vs40.79vs22.31, $P=0.042$). The expression of the MIA gene was related to the expression of PR in immunohistochemistry, and the expression of the MIA gene was high in PR-positive patients (median, 2.72vs0.65, $P=0.024$). Patients with low expression of NR3C2 tended to have positive Her-2 expression (median, 1.94 vs. 1.16, $P=0.016$) and Ki-67 ≥ 20% (median, 2.73 vs. 1.16, $P=0.009$). These 8 immune genes were not significantly different from whether the patient was menopausal, whether there was lymph node metastasis, and whether the ER expression was positive ($P>0.05$).

Correlation between DEIRGs and ultrasonic characteristics of breast cancer

The correlation between 8 immune-related genes and ultrasonic characteristics in clinically collected breast cancer patients is shown in Tables 4 and 5. In Table 4, we divided the patients into two groups according to the characteristics of B-mode ultrasound: whether the aspect ratio of the tumor is greater than or equal to 1, whether

Clinicopathological characteristics		CXCL2	MIA	NR3C2	PTX3	S100B	SAA1	SAA2	CXCL9
Age	≥60	0.45(0.26,0.98)	1.32(0.38,6.63)	2.19(0.86,3.56)	0.16(0.10,0.51)	0.62(0.17,1.86)	11.31(5.58,47.26)	0.89(0.24,2.84)	4.59(1.49,12.09)
	<60	0.79(0.53,1.28)	1.25(0.49,4.64)	1.32(0.86,2.47)	0.18(0.10, 0.37)	0.72(0.40,1.15)	14.79(8.36,31.87)	1.13(0.49,2.22)	26.31(8.88,61.00)
	95%CI	[-0.69,0.08]	[-2.55,2.78],	[-0.60,1.63]	[-0.11,0.16]	**[-0.56,0.63]**	[-11.38,15.08]	[-1.02,0.71]	**[-45.34,-3.56]**
	P value	0.101	0.46	0.442	0.757	**0.035**	0.782	0.546	**0.004**
Menopause	Yes	0.70(0.36,1.21)	1.02(0.38,5.45)	1.73(0.70,3.11)	0.19(0.09,0.38)	0.66(0.23,1.75)	12.96(6.69,31.25)	1.00(0.38,1.96)	12.51(2.83,44.51)
	No	0.72(0.50,1.16)	1.59(0.56,6.42)	1.16(0.88,2.19)	0.15(0.10,0.44)	0.72(0.42,0.98)	15.41(8.40,34.75)	1.60(0.45,2.35)	26.31(7.56,52.32)
	95%CI	[-0.41,0.28]	[-2.57,0.90]	[-0.67,1.23]	[-0.11,1.20]	[-0.41,0.49]	[-12.73,6.93]	[-1.11,0.54]	[-25.61,5.81]
	P value	0.633	0.553	0.874	0.965	0.942	0.613	0.613	0.317
Tumor size	≥20 mm	0.62(0.44,0.82)	0.88(0.33,3.65)	0.95(0.62,1.65)	0.15(0.08,0.30)	0.64(0.34,0.89)	13.14(7.87,23.69)	0.98(0.50,1.99)	33.92(9.06,58.64)
	<20 mm	1.15(0.36,2.02)	2.56(0.61,8.87)	2.63(1.52,4.02)	0.33(0.11,0.45)	0.92(0.39,2.02)	24.01(7.30,44.72)	1.60(0.38,3.73)	6.92(3.92,16.73)
	95%CI	[-1.10,0.11]	[-5.11,0.29]	**[-2.46,-0.57]**	[-0.25,0.40]	[-1.15,0.08]	[-22.95,4.76]	[-1.27,0.50]	[-1.35,37.91]
	P value	0.171	0.234	**0.001**	0.162	0.122	0.356	0.529	0.084
Positive lymph nodes	Yes	0.79(0.47,1.28)	1.10(0.43,3.59)	1.49(0.86,2.72)	0.28(0.11,0.43)	0.64(0.34,1.08)	14.11(6.69,24.26)	0.89(0.49,2.05)	14.14(4.17,61.00)
	No	0.66(0.33,1.09)	1.50(0.55,6.98)	1.48(0.88,3.13)	0.15(0.06,0.33)	0.74(0.41,1.84)	16.69(8.29,40.57)	1.66(0.34,2.43)	15.60(4.66,41.81)
	95%CI	[-0.23,0.47]	[-4.19,0.62]	[-0.99,0.65]	[-0.03,0.23]	[-0.71,0.19]	[-18.85,6.21]	[-1.2,0.46]	[-14.66,18.27]
	P value	0.478	0.409	0.696	0.206	0.361	0.633	0.553	0.828
TNM Stage	IA	0.60(0.31,1.36)	3.61(0.66,7.47)	2.46(1.33,4.55)	0.17(0.09,0.39)	0.76(0.49,1.84)	24.01(6.91,40.57)	1.70(0.40,2.60)	5.55(2.26,14.59)
	IIA	0.89(0.49,2.04)	0.89(0.35,9.10)	1.97(0.92,2.63)	0.20(0.10,0.45)	1.24(0.39,2.05)	11.72(7.56,60.91)	1.09(0.27,4.46)	40.79(6.76,111.49)
	IIB	0.59(0.45,0.80)	0.86(0.36,3.47)	0.93(0.57,1.53)	0.15(0.09,0.34)	0.52(0.21,0.73)	14.04(6.98,23.41)	0.91(0.55,1.66)	22.31(3.80,57.46)
	95%CI IA	[-0.43,3.50]	[-0.51,13.53]	**[1.55,4.38]**	[0.11,0.38]	**[0.30,2.24]**	[-6.24,89.04]	[-0.25,5.98]	**[1.99,18.60]**
	95%CI IIA	[0.59,2.58]	[0.99,8.95]	**[1.22,2.63]**	[0.15,0.38	**[0.73,1.91]**	[10.35,56.43]	[0.22,5.32]	**[-3.93,180.77]**
	95%CI IIB	[0.50,0.80]	[0.75,2.83]	**[0.38,2.94]**	[0.10,0.41]	**[0.31,0.70]**	[10.01,21.60]	[0.72,1.57]	**[13.89,42.06]**
	P value	0.247	0.302	**0.034**	0.828	**0.048**	0.776	0.729	**0.042**
ER	Positive	0.72(0.42,1.10)	1.47(0.43,4.64)	1.25(0.86,3.11)	0.17(0.10,0.38)	0.73(0.42,1.22)	14.11(8.20,31.87)	1.07(0.42,1.72)	14.14(5.05,44.51)
	Negative	0.70(0.34,1.29)	1.00(0.45,9.07)	1.75(1.14,2.54)	0.21(0.07,0.48)	0.40(0.18,2.00)	13.02(6.70,54.58)	2.11(0.37,4.27)	13.94(3.84,52.32)
	95%CI	[-0.33,0.47]	[-5.69,1.52]	[-1.13,0.89]	[-0.18,0.10]	[-0.39,0.60]	[-16.21,11.28]	[-2.06,0.30]	[-21.96,18.95]
	P value	0.858	0.708	0.683	0.832	0.503	0.987	0.272	0.883
PR	Positive	0.75(0.41,1.64)	2.72(0.85,5.37)	1.41(0.86,3.15)	0.18(0.11,0.420	0.74(0.52,1.60)	19.74(8.43,33.20)	1.14(0.47,1.76)	13.58(4.90,40.79)
	Negative	0.62(0.35,1.03)	0.65(0.36,6.58)	1.51(0.86,2.46)	0.15(0.08,0.38)	0.44(0.20,0.89)	9.24(5.90,24.54)	0.87(0.37,2.40)	22.31(3.92,57.46)
	95%CI	[-0.21,0.56]	**[-0.41,3.02]**	[-0.65,1.10]	[-0.12,0.12]	[-0.15,0.66]	[-2.38,17.35]	[-0.75,0.79]	[-30.65,9.66]
	P value	0.535	**0.024**	0.768	0.836	0.162	0.153	0.906	0.658
Her-2	Positive	0.61(0.34,0.90)	1.00(0.45,3.94)	1.16(0.86,1.63)	0.15(0.11,0.31)	0.72(0.42,0.89)	13.14(6.98,36.50)	1.70(0.50,2.71)	17.95(5.45,59.83)
	Negative	0.79(0.43,1.83)	2.53(0.34,5.89)	1.94(0.88,3.67)	0.23(0.09,0.43)	0.68(0.23,1.75)	14.86(8.23,31.97)	1.07(0.50,2.71)	14.14(2.83,42.76)
	95%CI	[-0.72,0.12]	[-3.03,0.69]	**[-1.92,0.22]**	[-0.20,0.06]	[-0.58,0.35]	[-12.35,8.36]	[-0.51,1.33]	[-10.47,23.50]
	P value	0.26	0.777	**0.016**	0.54	0.94	0.777	0.463	0.427
Ki-67	≥20%	0.66(0.44,0.96)	0.83(0.33,3.96)	1.16(0.71,2.11)	0.16(0.10,0.35)	0.69(0.33,1.07)	12.27(6.70,24.86)	0.96(0.35,1.92)	23.42(4.93,52.32)
	<20%	0.93(0.35,1.96)	3.60(1.31,9.46)	2.73(1.17,4.80)	0.26(0.07,0.45)	0.89(0.55,1.78)	25.84(9.88,39.18)	1.60(0.58,3.88)	9.84(3.10,32.79)
	95%CI	[-0.92,0.24]	[-5.01,0.09]	**[-2.80,-0.29]**	[-0.24,0.09]	[-0.82,0.19]	[-24.91,1.12]	[-1.55,0.18]	[-4.33,31.98]
	P value	0.447	0.053	**0.009**	0.631	0.312	0.076	0.137	0.243

Table 3. Correlation between DEIRGs and clinical characteristics. Data refers to the numbers of subject included medians and quartiles (M (Q1, Q2)) for continuous variables. P values indicate comparisons between two groups using the Mann-Whitney U test, Kolmogorov-Smirnov, or Moses extreme reaction test and multiple independent samples using the Kruskal–Wallis test. ER estrogen receptor, PR progesterone receptor, HER-2 human epidermal growth factor receptor. Significant values are in bold.

there are edge burrs, and whether there is calcification, and analyzed whether the immune-related genes were differentially expressed in the two groups. In Table 5, the correlation of two continuous variables between the expression of immune genes and the characteristics of microvascular ultrasound, shear wave elastography, and contrast-enhanced ultrasound was analyzed.

Data refers to the numbers of subject included medians and quartiles (M (Q1, Q2)) for continuous variables P values indicate comparisons between two groups using the Mann-Whitney U test, Kolmogorov-Smirnov, or Moses extreme reaction test.

The SAA2 gene was associated with the presence of edge burrs, and the SAA2 expression was low in tumors with edge burrs (median, 1.05 vs. 2.03, $P = 0.04$). Edge burrs on B-mode ultrasound predict tumor invasion,

Ultrasonic characteristics		CXCL2	MIA	NR3C2	PTX3	S100B	SAA1	SAA2	CXCL9
Edge burrs	Yes	0.69(0.41,1.19)	1.16(0.53,4.33)	1.41(0.86,3.08)	0.15(0.08,0.40)	0.66(0.32,1.09)	14.04(7.56,30.67)	1.05(0.38,1.75)	14.06(5.08,42.11)
	No	0.89(0.42,1.50)	6.77(0.31,10.54)	1.99(1.11,2.46)	0.35(0.16,0.44)	1.80(0.67,2.72)	25.81(8.11,89.07)	2.03(1.22,10.64)	50.61(2.73,319.57)
	95%CI	[-0.59,0.47]	[-6.95,1.52]	[-1.35,1.26]	[-0.27,0.09]	[-1.74,0.08]	[-65.22,7.55]	**[-5.95,-0.09]**	[-64.42,12.68]
	P value	0.769	0.449	0.802	0.252	0.056	0.331	**0.04**	0.501
Aspect ratio	>1	0.63(0.41,0.92)	1.78(0.70,6.67)	1.09(0.79,2.46)	0.15(0.10,0.36)	0.74(0.41,1.38)	14.04(7.57,35.84)	1.09(0.48,1.95)	24.53(4.41,54.03)
	≤1	1.10(0.46,1.77)	0.66(0.33,3.50)	1.97(1.19,3.92)	0.20(0.09,0.45)	0.62(0.27,1.60)	16.79(7.70,30.67)	1.13(0.37,2.49)	10.77(4.54,30.75)
	95%CI	[-0.87,0.17]	[-0.34,3.39]	[-1.97,0.12]	[-0.15,0.09]	[-0.33,0.54]	[-9.81,11.38]	[-0.68,0.94]	[-4.69,32.65]
	P value	0.234	0.199	0.104	0.627	0.523	0.976	0.605	0.345
Calcification	Yes	0.63(0.32,1.09)	1.34(0.23,5.76)	0.98(0.79,2.63)	0.20(0.11,0.46)	0.72(0.32,1.38)	9.45(5.50,20.04)	0.87(0.32,2.14)	11.44(3.69,47.74)
	No	0.75(0.47,1.46)	1.16(0.55,5.71)	1.53(1.03,3.08)	0.16(0.07,0.38)	0.73(0.43,1.52)	22.21(8.38,35.84)	1.54(0.52,2.18)	17.62(5.54,52.80)
	95%CI	[-0.48,0.22]	[-1.7,1.54]	[-1.11,0.52]	[-0.09,0.13]	[-0.50,0.26]	[-19.04,1.45]	[-1.16,0.34]	[-18.39,11.72]
	P value	0.467	0.728	0.337	0.581	0.622	0.128	0.243	0.45

Table 4. Correlation between immune-related genes and B-mode ultrasonic characteristics. Significant values are in bold.

Ultrasonic characteristics		CXCL2	MIA	NR3C2	PTX3	S100B	SAA1	SAA2	CXCL9
CDFI-CPP	*r*	-0.113	0.145	-0.052	-0.037	0.033	0.238	0.243	-0.143
	95%CI	[-0.46,0.21]	[-0.18,0.48]	[-0.37,0.28]	[-0.35,0.27]	[-0.31,0.38]	[-0.12,0.54]	[-0.08,0.53]	[-0.50,0.21]
	P value	0.500	0.384	0.757	0.826	0.845	0.150	0.142	0.391
UMA-CPP	*r*	-0.229	-0.040	0.002	-0.221	-0.006	0.077	0.141	0.166
	95%CI	[-0.54,0.11]	[-0.38,0.29]	[-0.30,0.33]	[-0.53,0.11]	[-0.38,0.32]	[-0.26,0.42	[-0.21,0.47]	[-0.19,0.47]
	P value	0.166	0.811	0.991	0.182	0.969	0.644	0.399	0.320
E_{mean}	*r*	0.025	0.151	-0.140	-0.197	0.059	0.045	-0.040	0.195
	95%CI	[-0.34,0.36]	[-0.18,0.43]	[-0.45,0.20]	[-0.50,0.13]	[-0.27,0.39]	[-0.27,0.38]	[-0.38,0.37]	[-0.14,0.49]
	P value	0.882	0.365	0.403	0.235	0.724	0.787	0.809	0.241
E_{max}	*r*	– 0.240	0.007	-0.311	**-0.346**	-0.075	-0.177	-0.229	0.217
	95%CI	[– 0.59,0.15]	[– 0.35,0.32]	[-0.62,0.06]	**[-0.64,0.001]**	[-0.42,0.29]	[-0.48,0.15]	[-0.54,0.16]	[-0.14,0.54]
	P value	0.146	0.967	0.057	**0.033**	0.654	0.288	0.167	0.191
E_{min}	*r*	0.104	-0.090	0.048	-0.132	-0.082	-0.031	-0.007	0.107
	95%CI	[-0.24,0.44]	[-0.48,0.27]	[-0.30,0.37]	[-0.41,0.19]	[-0.44,0.29]	[-0.38,0.30]	[-0.35,0.34]	[-0.25,0.46]
	P value	0.533	0.589	0.776	0.429	0.625	0.855	0.965	0.522
E_{sd}	*r*	-0.124	0.068	-0.242	0.296	-0.008	-0.128	-0.186	0.220
	95%CI	[-0.48,0.25]	[-0.23,0.39]	[-0.54,0.12]	[-0.58,0.05]	[-0.34,0.35]	[-0.42,0.22]	[-0.50,0.16]	[-0.12,0.51]
	P value	0.460	0.684	0.144	0.071	0.964	0.445	0.263	0.185
PkI	*r*	-0.141	-0.083	**-0.450**	**-0.347**	-0.217	-0.133	-0.083	0.256
	95%CI	[-0.44,0.18]	[-0.41,0.25]	**[-0.68,-0.15]**	**[-0.59,-0.04]**	[-0.51,0.10]	[-0.47,0.22]	[-0.40,0.23]	[-0.12,0.58]
	P value	0.399	0.619	**0.005**	**0.033**	0.191	0.427	0.621	0.121
AUC	*r*	-0.063	-0.007	**-0.390**	-0.300	-0.184	-0.075	-0.033	0.213
	95%CI	[-0.40,0.29]	[-0.34,0.33]	**[-0.66,-0.05]**	[-0.57,0.02]	[-0.51,0.16]	[-0.42,0.28]	[-0.36,0.30]	[-0.13,0.53]
	P value	0.709	0.968	**0.015**	0.067	0.270	0.656	0.842	0.198
AT	*r*	0.019	0.072	**0.407**	0.235	0.071	0.120	0.099	-0.147
	95%CI	[-0.35,0.38]	[-0.29,0.43]	**[0.11,0.65]**	[-0.07,0.49]	[-0.29,0.42]	[-024,0.47]	[-0.27,0.46]	[-0.45,0.19]
	P value	0.908	0.669	**0.011**	0.155	0.873	0.474	0.555	0.377
TTP	*r*	0.010	0.032	**0.384**	0.221	0.012	0.126	0.139	-0.190
	95%CI	[-0.34,0.37]	[-0.35,0.39]	**[0.10,0.45]**	[-0.07,0.49]	[-0.35,0.35]	[-026,0.49]	[-0.21,0.47]	[-0.49,0.15]
	P value	0.954	0.850	**0.017**	0.183	0.943	451.000	0.404	0.252

Table 5. Correlation between DEIRGs and microvascular ultrasound, SWE, and CEUS. P values indicate comparisons between two groups using Spearman correlation analysis. r indicate correlation coefficient between the two groups. Significant values are in bold.

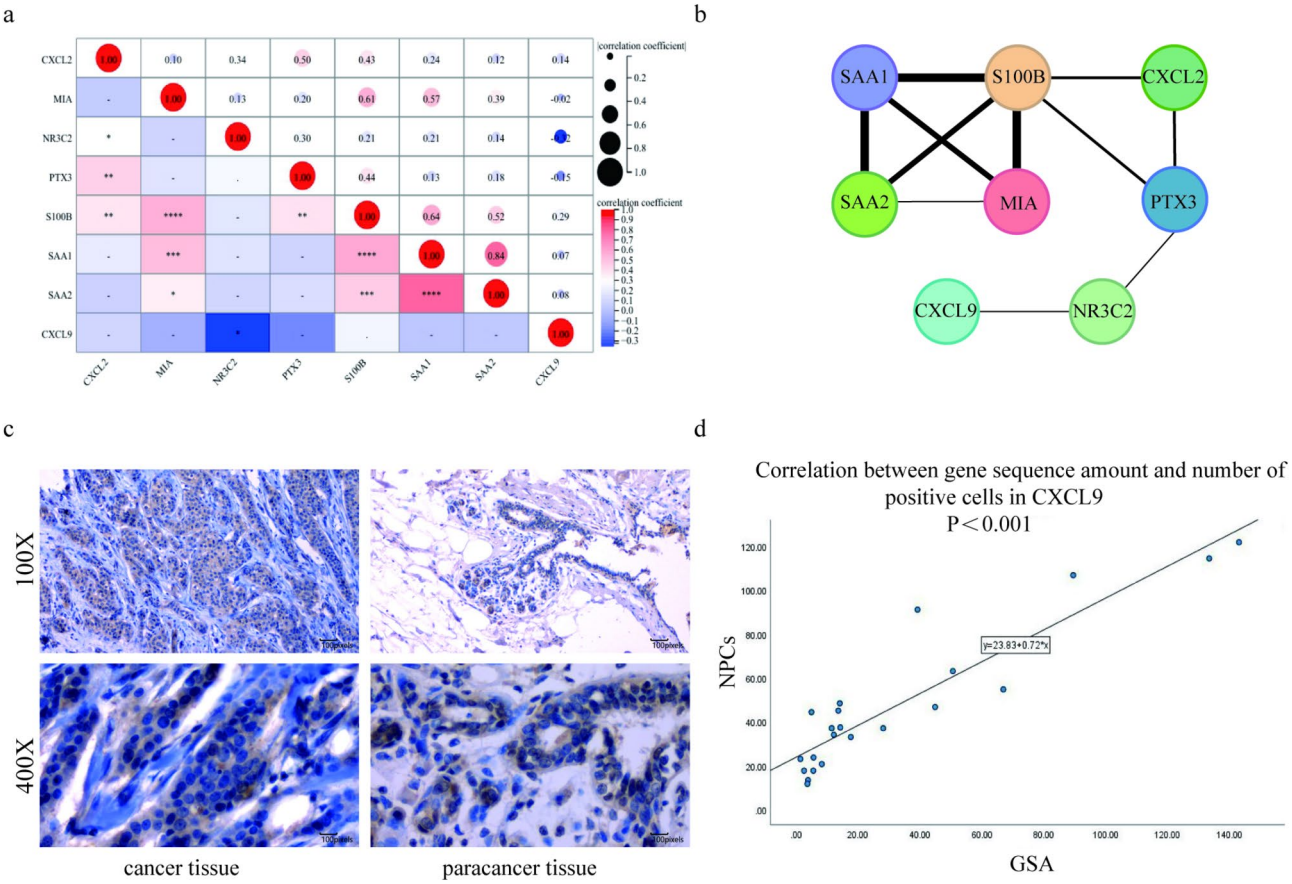

Fig. 4. Correlation analysis between immune genes and expression products. (**a**) Correlation heat map. (**b**) Correlation network diagram. The thicker the line between genes, the greater the correlation coefficient. (**c**) Immunohistochemical staining of CXCL9 in cancer and adjacent tissues. Left: strong positive in cancer, right: weak positive in adjacent tissues. (**d**) Scatter plot and fitting line equation of CXCL9 sequencing amount and number of positive cells in immunohistochemical staining.

so tumors with low SAA2 expression may have stronger peripheral invasion and predict a worse prognosis for patients, which is consistent with SAA2 expression in public databases. Whether the aspect ratio of the tumor was greater than 1 and whether there was calcification inside the tumor were not correlated with these 8 immune-related genes ($P > 0.05$). In the linear correlation analysis between SWE and immune genes, PTX3 had a linear correlation with E_{max} (r=-0.346, $P = 0.033$), and the two were negatively correlated. Emax indicates the maximum hardness of the tumor, and the tumors of patients with low PTX3 expression tend to have greater hardness. The greater hardness predicts the worse prognosis of patients, which is consistent with the expression of PTX3 in public databases. In CEUS, PKI values were negatively correlated with the expression levels of NR3C2 (r=-0.450, $P = 0.005$) and PTX3 (r=-0.347, $P = 0.033$). Tumors with low expression of NR3C2 and PTX3 had higher peak intensity in CEUS, and the higher the peak intensity, the better the blood supply of the tumor, indicating the worse prognosis of the patient, which was consistent with the expression of NR3C2 and PTX3 in the public database. NR3C2 expression was also negatively correlated with AUC (r=-0.390, $P = 0.015$), and positively correlated with AT ($r = 0.407$, $P = 0.011$) and TTP ($r = 0.384$, $P = 0.017$). This suggested that tumors with low NR3C2 expression also had a larger area under the curve, longer contrast agent development time, and longer time to peak in CEUS, all of which suggested better tumor blood supply and poorer patient prognosis. There was no linear correlation between the expression of these 8 immune-related genes and the remaining ultrasound parameters($r < 0.3$, $P > 0.05$).

The correlation between DEIRGs and expression products

Since some ultrasound and clinical characteristics are related to a variety of immune-related genes, we performed correlation analysis on the expression levels of these 8 immune-related genes and plotted heat maps (Fig. 4a). The expression of CXCL2 was related to PTX3 and S100B. The expression of NR3C2 was related to PTX3 and CXCL9. We used the network diagram to represent the correlation between genes, and found that the expression levels of some genes were correlated, which was conducive to the subsequent multiple analysis (Fig. 4b). Previous studies have shown that CXCL9 is overexpressed in breast cancer, which is associated with some prognostic factors such as negative lymph nodes, small tumor size, and low proliferation index, which is consistent with our findings[29]. The low expression of CXCL9 can also change the tumor microenvironment, promote the

differentiation of macrophages M1 into M2, regulating the breast cancer immunotherapy[30]. Therefore, anti-CXCL9 immunohistochemical staining was performed on the paraffin pathological sections of the patient's carcinoma and adjacent tissue to analyze the gene expression products, and the adjacent breast tissue was used as a negative control. Immunohistochemical results showed that the expression of CXCL9 in breast cancer tissues was stronger than that in adjacent breast tissues, with statistical difference ($P < 0.05$) (Fig. 4c). SPSS was used to analyze the relationship between CXCL9 gene sequencing amount (GSA) and the number of positive cells (NPCs) obtained by immunohistochemical staining, indicating that there was a significant correlation between CXCL9 GSA and NPCs ($P < 0.001$). A correlation scatter plot and linear equation is shown in Fig. 4d.

Discussion

The diagnostic criteria of breast cancer are tumor pathology and molecular classification, which can predict the prognosis of patients, but the tumor pathological tissue has a selection bias through invasive tissue sampling. However, radiomics reflects the overall information of the tumor, so it is worth studying. Previously, many studies have used radiogenomics to screen differentially expressed genes in breast cancer by using breast ultrasound or breast NMR[12,31]. A large number of radiomics studies based on breast ultrasound and NMR analyzed the correlation between radiological characteristics and clinical characteristics, so as to use certain radiological characteristics to predict the clinical characteristics, such as the NMR characteristics of breast cancer to predict axillary lymph node metastasis[32]. It has been reported that predictive models of clinical characteristics were constructed by radiomics. For example, Ioana et al. used the contrax-enhanced ultrasonic characteristics of breast cancer and the expression of HR, HER-2 and Ki-67 to construct predictive models[33]. Compared with breast MRI, ultrasound features have the advantages of non-invasive, easy to obtain, simple operation and good patient compliance. The role of immune-related genes in cancer has also been extensively studied, which has an influence of the tumor immune microenvironment and the efficacy of immunotherapy to improve patient prognosis[34,35]. Some studies identified immune-related genes associated with the immune microenvironment of breast cancer through sequencing datasets in public databases, such as single-cell sequencing datasets and ordinary transcriptome data, to establish prognostic models and predict cancer risk[36,37]. Our study collected comprehensive ultrasonic characteristics of breast cancer and performed whole transcriptome sequencing of the tumor. The immune-related genes were screened by public databases, and their correlation with clinical characteristics and ultrasonic characteristics of tumors was analyzed. The immune-related genes were further screened to explore the predictive effect of ultrasonic characteristics on the overall survival and prognosis of breast cancer patients and the guiding value in subsequent treatment. Therefore, our research plan is different from the past research and is innovative.

Our study found that the expression of immune-related genes was related to the clinical and ultrasonic characteristics of breast cancer patients. In the correlation analysis with clinical characteristics, NR3C2 expression was associated with tumor size, TNM stage, Her-2, and Ki-67, MIA was associated with PR expression, and S100B and CXCL9 were associated with age and TNM stage of patients. This suggests that the expression of these genes can affect the stage and molecular typing of patients, thus affecting the survival and prognosis of patients. Patients aged ≥ 60 years and those with a later stage had lower S100B and CXCL9 gene expression, predicting worse survival. In the correlation analysis with ultrasonic characteristics, SAA2 was related to the presence or absence of edge burrs. NR3C2 was correlated with CEU parameters, including PKI, AUC, AT, and TTP. PTX3 was also associated with E_{max} and PKI. These parameters have predictive value for the expression of immune genes in patients and can predict tumor prognosis and develop more accurate treatment plans. Therefore, when the peak intensity and the area under the curve are larger, the contrast agent development time and time to peak are shorter, and the expression of the NR3C2 gene is lower. The lower the expression of NR3C2, the larger the tumor size, the later the TNM stage, Her-2 tends to be positive, and the higher the expression of Ki-67. It prompts us to predict the expression of NR3C2 by CEUS, and then predict the stage and type of tumor. We can also detect the expression of NR3C2 in advanced or Her-2 positive or high Ki-67 expression breast cancer, to guide the follow-up treatment of breast cancer patients. In future studies, we can explore a new therapeutic approach to increase NR3C2 gene expression.

Our study shows that PKI, AUC, AT, and TTP can predict the expression of NR3C2 and can be used to guide subsequent treatment. The expression products of immune-related genes, such as chemokines, can promote tumor angiogenesis[38]. These new tumor vessels showed higher peak intensity and areas under the curve on breast ultrasound, faster contrast agent development time and time to peak, so we believe that CEUS can be used to select immunotherapy. Breast cancer is a highly heterogeneous malignant tumor, but the treatment of breast cancer now mainly depends on the results of immunohistochemistry. Breast ultrasound can focus on the overall situation of the tumor. Our study predicted the expression of immune genes through macroscopic ultrasonic characteristics to guide the follow-up treatment of breast cancer. For example, the positive expression of Her-2 is associated with low expression of NR3C2. Therefore, in the treatment of Her-2 positive breast cancer, in addition to conventional chemotherapy and targeted therapy, we can use a new treatment method to promote the expression of NR3C2 to improve the overall survival of patients. Our study not only screened IRGs that can predict the prognosis of patients, but also explored the ultrasonic characteristics associated with the expression of these genes. This is conducive to the diagnosis of breast cancer, the choice of treatment methods, and the prediction of patient survival in the future, to formulate accurate individualized monitoring and treatment plans for patients. Because of the low incidence of breast cancer in men, male patients were not included in our study, but our findings are equally applicable to male patients. Male breast cancer patients also have corresponding clinical and ultrasonic characteristics, which can predict the amount of gene expression to guide the personalized treatment of male patients.

Endothelial cells are the basic components of blood vessels. Endothelial cell proliferation is conducive to the formation of new blood vessels, so it is a good target for predicting angiogenesis. Dysfunction of

neovascularization is associated with cancer, inflammation, and immune disorders[39]. It has been reported that the interaction between breast cancer cells and tumor endothelial cells can induce tumor angiogenesis and regulate the immune response in the tumor microenvironment, such as promoting the secretion of immune regulatory factors[40]. A large number of studies have shown that infiltrating immune cell subsets in the tumor microenvironment can regulate tumor angiogenesis and remodeling[41]. Our study found that the blood flow characteristics observed by CEUS may predict the expression of immune-related genes in tumors. Abnormal expression of immune-related genes can also affect tumor angiogenesis, which is manifested in CEUS changes consistent with previous research results. Therefore, we found that there was a correlation between CEUS and IRGs in breast cancer. CEUS can be used as a promising imaging biomarker to predict the prognosis and treatment strategies of tumor patients.

Nowadays, immunotherapy, especially immune checkpoint inhibitors, has gradually attracted people's attention in improving the overall survival of breast cancer, but drug resistance continues to occur, and we need to continue to explore immunotherapy targets with better treatment and prediction effects[42]. Recently, a large number of studies have been exploring new immunotherapy targets. For instance, Liu et al. have reported that RAD51, TRPM7 and other genes are closely related to tumor immune microenvironment, drug sensitivity and tumor immunity in some cancers, which can be used as potential immunotherapy targets[43,44]. Voltage-gated sodium channels (VGSCs) genes and cuproptosis genes play an important role in the diagnosis and treatment of some cancers and are potential therapeutic pathways[45,46]. CXCL2 (C-X-C motif chemokine ligand 2) is lowly expressed in breast cancer, and it has been proved that inhibiting CXCL2 can promote the proliferation and lung metastasis of breast cancer[47,48]. In our study, CXCL2 was correlated with the expression levels of MIA and NR3C2, but no correlation with clinical and ultrasonic characteristics was observed. The role of MIA (MIA SH3 domain containing) in breast cancer has not been studied experimentally, but in esophageal cancer, MIA can be used as a immunotherapy target for the prognosis of poorly differentiated esophageal cancer[49]. The high expression of MIA is associated with PR positive in breast cancer immunohistochemistry. A large number of studies have shown that NR3C2 (Nuclear receptor subfamily 3 group C member 2) is lowly expressed in breast cancer compared with normal tissues. It is a potential prognostic biomarker and is related to the choice of subsequent treatment options for patients[50]. Studies have shown that miR-301b-3p can target NR3C2, thereby promoting the proliferation, migration, and invasion of breast cancer cells[51]. In our study, the low expression of NR3C2 was associated with tumor size ≥ 20 mm, later TNM stage, Her-2 positive, and Ki-67 ≥ 20% in clinical characteristics. It was negatively correlated with PKI and AUC in CEUS, and positively correlated with AT and TTP, indicating that the low expression of NR3C2 was associated with more abundant tumor blood vessels, which was consistent with previous research conclusions. Therefore, we believe that the role of NR3C2 in breast cancer can be further studied as an immunotherapy target and can be predicted by ultrasonic characteristics. Moreover, tumors with larger size, later TNM stage, positive HER-2 and Ki-67 ≥ 20% may exhibit characteristics of high PKI and AUC and low AT and TTP under CEUS, indicating more tumor angiogenesis. PTX3 (Pentraxin 3) is an immune-related gene. Its expression product PTX3 protein has innate immune function and angiogenesis, which can inhibit or promote angiogenesis[52]. Studies have shown that the expression level of PTX3 is associated with breast cancer staging. Overexpression of PTX3 promotes tumor invasion, proliferation, and stemness[53,54]. In our study, the expression of the PTX3 gene was negatively correlated with the Emax of shear wave elastography, indicating that the higher the expression of the PTX3, the lower the maximum hardness of the tumor. The expression of PTX3 was also negatively correlated with the value of PKI in CEUS, indicating that high expression of PTX3 could inhibit vascular function. Studies have shown that high expression of S100B (S100 calcium binding protein B) can inhibit the metastasis of ER-negative breast cancer and is an immunotherapy target for predicting breast cancer metastasis[55]. In our study, patients with low expression of S100B were older (≥ 60 years) and later TNM stage. In triple-negative breast cancer, SAA1 (serum amyloid A1) expression is associated with invasiveness, cancer-associated adipocyte infiltration, inflammation, lipolysis, tumor stemness, and tumor microenvironment[56]. In our study, SAA1 was correlated with the expression levels of SAA2, MIA and S100B, but no correlation with clinical and ultrasonic characteristics was observed. There is no research on SAA2 (serum amyloid A2) in breast cancer, but the SAA gene expression product is synthesized by cytokines released by activated monocytes and macrophages[57]. Our study found that SAA2 was associated with the presence or absence of edge burrs by B-mode ultrasound. Studies have shown that CXCL9 (C-X-C motif chemokine ligand 9) can stimulate the JAK/STAT signaling pathway and is an immunotherapy target for the prognosis and efficacy of immunotherapy in patients with triple negative breast cancer[30,58]. In this study, the expression of the CXCL9 gene was also statistically different from the age of onset and TNM stage. The immune-related genes screened in our study are related to the clinical and ultrasonic characteristics of patients, and are potential immunotherapy targets for breast cancer. We can predict the expression of certain immune-related genes based on ultrasonic characteristics, so as to guide personalized immunotherapy and predict the overall survival of patients.

Our study had several limitations. First, the number of breast cancer patients included was small. Among the 38 patients included, only 3 were triple-negative breast cancer. The number was relatively small and non-parametric tests for multiple independent samples could not be performed, so some statistical results were missing. And the 38 cases of breast cancer pathology results were invasive ductal carcinoma, pathological type was single. Next, we can further expand the research sample and conduct validation studies through multi-center cooperation and sharing data with other researchers to improve the credibility of the research. Second, there was a data bias. In the inclusion and exclusion criteria of our study, patients with distant metastasis were excluded. Therefore, our results may not apply to all breast cancers, and further studies are needed to expand the number of cases. The inevitable bleeding, necrosis and fat composition in sequenced tumor tissues may affect whole transcriptome sequencing. Due to the different degree of cooperation with patients, there may be subjective influence in the process of data collection. Third, there are few classifications of ultrasonic characteristics and direct correlation analysis of numerical variables. We believe that further processing and classification of these

values can lead to more clear conclusions. Fourth, there was no correlation analysis between the protein of gene expression product and the clinical and ultrasonic characteristics of patients, and further research can be carried out after expanding the database.

Conclusions

The expression of immune-related genes was related to the clinical characteristics of breast cancer patients, such as age of onset and TNM stage. The detection of immune-related genes in patients who meet these characteristics is conducive to the development of personalized precision treatment, and greatly improving the prognosis of patients. Immune-related genes can be predicted by ultrasonic characteristics, such as the presence of edge burrs, the Emax value of shear wave elastography, and CEUS including PKI, AUC, AT, and TTP. These ultrasonic characteristics can be used to predict the expression of certain immune-related genes in patients, to predict the survival and recurrence of breast cancer patients, and to monitor the expression of genes in tumors. Therefore, the use of ultrasonic characteristics to predict the expression of immune-related genes helps to identify potential immunotherapy targets and develop personalized treatment for patients. In the future, we can study the in-depth mechanisms of these genes in the breast cancer angiogenesis and immune microenvironment. In addition, this line of research can be applied to other cancers to explore the correlation between genes and ultrasonic characteristics in other cancers.

Data availability

The results of this study are partially based on data available at the GEO (https://www.ncbi.nlm.nih.gov/geo/) and IMMPORT Shared Data (https://www.immport.org/home). The whole transcriptome sequencing datasets have not yet reached the stage of being made public. However, author Tingyao Dou can be contacted on reasonable request at tingyao625@163.com.

Received: 23 October 2024; Accepted: 2 May 2025
Published online: 07 May 2025

References

1. Siegel, R. L., Giaquinto, A. N., Jemal, A. & Cancer statistics *CA: A Cancer Journal for Clinicians* 74, 12–49, (2024). https://doi.org/10.3322/caac.21820 (2024).
2. Maughan, K. L., Lutterbie, M. A., & Ham, P. S. Treatment of breast cancer. *Am Fam Physician*. **81**, 1339–1346 (2010).
3. Sonkin, D., Thomas, A., & Teicher, B. A. Cancer treatments: Past, present, and future. *Cancer Genet*. **286-287**, 18–24. https://doi.org/10.1016/j.cancergen.2024.06.002 (2024).
4. Guo, R., Lu, G., Qin, B. & Fei, B. Ultrasound imaging technologies for breast Cancer detection and management: A review. *Ultrasound. Med. Biol.* **44**, 37–70. https://doi.org/10.1016/j.ultrasmedbio.2017.09.012 (2018).
5. Chen, M., Li, B., & Liu, H. V-blade tip needle scalpel reducing surgery time in ultrasonography-guided percutaneous A1 pulley release. *Asian J Surg*. **S1015-9584**, 01749-4. https://doi.org/10.1016/j.asjsur.2024.08.011 (2024).
6. Chang, D. H., & Shu, Y. L. Clinic efficacy and safety of ultrasound-guided Mammotome-assisted surgery for patients with breast benign tumors. *Eur Rev Med Pharmacol Sci*. **27**, 5985–5992. https://doi.org/10.26355/eurrev_202307_32950 (2023).
7. Cui, H. et al. Radiogenomic analysis of prediction HER2 status in breast cancer by linking ultrasound radiomic feature module with biological functions. *J. Translational Med.* **21** https://doi.org/10.1186/s12967-022-03840-7 (2023).
8. Bene, I. et al. Radiomic signatures derived from hybrid Contrast-Enhanced ultrasound images (CEUS) for the assessment of histological characteristics of breast cancer: A pilot study. *Cancers* **14**, 3905. https://doi.org/10.3390/cancers14163905 (2022).
9. Yoo, J. et al. Tumor stiffness measured by shear wave elastography correlates with tumor hypoxia as well as histologic biomarkers in breast cancer. *Cancer Imaging*. **20** https://doi.org/10.1186/s40644-020-00362-7 (2020).
10. Story, M. D., Durante, M. & Radiogenomics *Med. Phys.* **45**, doi:https://doi.org/10.1002/mp.13064 (2018).
11. Grimm, L. J. & Mazurowski, M. A. Breast Cancer radiogenomics: current status and future directions. *Acad. Radiol.* **27**, 39–46. https://doi.org/10.1016/j.acra.2019.09.012 (2020).
12. Bismeijer, T. et al. Radiogenomic analysis of breast Cancer by linking MRI phenotypes with tumor gene expression. *Radiology* **296**, 277–287. https://doi.org/10.1148/radiol.2020191453 (2020).
13. Yeh, A. C. et al. Radiogenomics of breast cancer using dynamic contrast enhanced MRI and gene expression profiling. *Cancer Imaging*. **19** https://doi.org/10.1186/s40644-019-0233-5 (2019).
14. Willsmore, Z. N. et al. Combined anti-PD-1 and anti-CTLA-4 checkpoint Blockade: treatment of melanoma and immune mechanisms of action. *Eur. J. Immunol.* **51**, 544–556. https://doi.org/10.1002/eji.202048747 (2021).
15. Nencioni, A. et al. The use of dendritic cells in cancer immunotherapy. *Crit. Rev. Oncol. Hematol.* **65**, 191–199. https://doi.org/10.1016/j.critrevonc.2007.10.002 (2008).
16. Zong, L. et al. Expression of the immune checkpoint VISTA in breast cancer. *Cancer Immunol. Immunother.* **69**, 1437–1446. https://doi.org/10.1007/s00262-020-02554-3 (2020).
17. Tang, L. et al. Expression and clinical significance of TIGIT in primary breast Cancer. *Int. J. Gen. Med. Volume*. **16**, 2405–2417. https://doi.org/10.2147/ijgm.s407725 (2023).
18. de Pulido, M. TIM-3 regulates CD103 + Dendritic cell function and response to chemotherapy in breast Cancer. *Cancer Cell.* **33**, 60–74e66. https://doi.org/10.1016/j.ccell.2017.11.019 (2018).
19. Edgar, R. Gene expression omnibus: NCBI gene expression and hybridization array data repository. *Nucleic Acids Res.* **30**, 207–210. https://doi.org/10.1093/nar/30.1.207 (2002).
20. Barrett, T. et al. NCBI GEO: archive for functional genomics data sets—update. *Nucleic Acids Res.* **41**, D991–D995. https://doi.org/10.1093/nar/gks1193 (2012).
21. Ritchie, M. E. et al. Limma powers differential expression analyses for RNA-sequencing and microarray studies. *Nucleic Acids Res.* **43**, e47–e47. https://doi.org/10.1093/nar/gkv007 (2015).
22. Bhattacharya, S. et al. ImmPort, toward repurposing of open access immunological assay data for translational and clinical research. *Sci. Data*. **5** https://doi.org/10.1038/sdata.2018.15 (2018).
23. Tang, Z. et al. GEPIA: a web server for cancer and normal gene expression profiling and interactive analyses. *Nucleic Acids Res.* **45**, W98–W102. https://doi.org/10.1093/nar/gkx247 (2017).
24. Kishore, J., Goel, M. & Khanna, P. Understanding survival analysis: Kaplan-Meier estimate. *Int. J. Ayurveda Res.* **1**, 274. https://doi.org/10.4103/0974-7788.76794 (2010).

25. Shi, X. Q., Li, J. L., Wan, W. B. & Huang, Y. A. Set of shear wave elastography quantitative parameters combined with ultrasound BI-RADS to assess benign and malignant breast lesions. *Ultrasound. Med. Biol.* **41**, 960–966. https://doi.org/10.1016/j.ultrasmedbio.2014.11.014 (2015).
26. Kristiansen, M. U., Martiniussen, M. A. & Larsen, A. S. F. Contrast-enhanced ultrasound of breast tumors: an initial experience. *Acta Radiol. Open.* **11**, 205846012210974. https://doi.org/10.1177/20584601221097458 (2022).
27. Shen, W. et al. Sangerbox: A comprehensive, interaction-friendly clinical bioinformatics analysis platform. *iMeta* 1, e36, (2022). https://doi.org/10.1002/imt2.36
28. Shen, W. et al. Sangerbox: A comprehensive, interaction-friendly clinical bioinformatics analysis platform. *iMeta*, **1**, e36. https://doi.org/10.1002/imt2.36 (2022).
29. Narita, D. et al. Altered levels of plasma chemokines in breast cancer and their association with clinical and pathological characteristics. *Neoplasma*, **63**, 141–149. https://doi.org/10.4149/neo_2016_017 (2016).
30. Wu, L. et al. CXCL9 influences the tumor immune microenvironment by stimulating JAK/STAT pathway in triple-negative breast cancer. *Cancer Immunol. Immunother.* **72**, 1479–1492. https://doi.org/10.1007/s00262-022-03343-w (2022).
31. Park, A. Y. et al. Radiogenomic analysis of breast Cancer by using B-Mode and vascular US and RNA sequencing. *Radiology* **295**, 24–34. https://doi.org/10.1148/radiol.2020191368 (2020).
32. Yu, Y. et al. Magnetic resonance imaging radiomics predicts preoperative axillary lymph node metastasis to support surgical decisions and is associated with tumor microenvironment in invasive breast cancer: A machine learning, multicenter study. *EBioMedicine*, **69**, 103460. https://doi.org/10.1016/j.ebiom.2021.103460 (2021).
33. Bene, I. et al. Radiomic Signatures Derived from Hybrid Contrast-Enhanced Ultrasound Images (CEUS) for the Assessment of Histological Characteristics of Breast Cancer: A Pilot Study. *Cancers*, **14**, 3905. https://doi.org/10.3390/cancers14163905 (2022).
34. Liu, H. Expression and potential immune involvement of cuproptosis in kidney renal clear cell carcinoma. *Cancer Genet*. **274-275**, 21-25. https://doi.org/10.1016/j.cancergen.2023.03.002 (2023).
35. Liu, H., & Tang, T. A bioinformatic study of IGFBPs in glioma regarding their diagnostic, prognostic, and therapeutic prediction value. *Am J Transl Res.* **15**, 2140-2155. (2023).
36. Liu, H., Dong, A., Rasteh, A. M., Wang, P., & Weng, J. Identification of the novel exhausted T cell $CD8^+$ markers in breast cancer. *Sci Rep*. **14**, 19142. https://doi.org/10.1038/s41598-024-70184-1 (2024).
37. Jiang, J., Yin, B., Luo, X., Chen, Y., & Wei, C. Genetic analysis uncovers potential mechanisms linking juvenile ldiopathic arthritisto breast cancer: A Bioinformatic Pilot study. *Cancer Genet*. **290-291**, 51-55. https://doi.org/10.1016/j.cancergen.2024.09.004 (2025).
38. Strieter, R. M. et al. Cancer CXC chemokine networks and tumour angiogenesis. *Eur. J. Cancer*. **42**, 768–778. https://doi.org/10.1016/j.ejca.2006.01.006 (2006).
39. Naito, H., Iba, T. & Takakura, N. Mechanisms of new blood-vessel formation and proliferative heterogeneity of endothelial cells. *Int. Immunol.* **32**, 295–305. https://doi.org/10.1093/intimm/dxaa008 (2020).
40. Terceiro, L. E. L. et al. The breast tumor microenvironment: A key player in metastatic spread. *Cancers* **13**, 4798. https://doi.org/10.3390/cancers13194798 (2021).
41. Stockmann, C., Schadendorf, D., Klose, R. & Helfrich, I. The impact of the immune system on tumor: angiogenesis and vascular remodeling. *Front. Oncol.* **4** https://doi.org/10.3389/fonc.2014.00069 (2014).
42. Wong, R. S., Ong, R. J., & Lim, J. S. Immune checkpoint inhibitors in breast cancer: development, mechanisms of resistance and potential management strategies. *Cancer Drug Resist*. **6**, 768-787. https://doi.org/10.20517/cdr.2023.58 (2023).
43. Liu, H., & Weng, J. A Pan-Cancer Bioinformatic Analysis of RAD51 Regarding the Values for Diagnosis, Prognosis, and Therapeutic Prediction. *Front Oncol*. **12**, 858756. https://doi.org/10.3389/fonc.2022.858756 (2022).
44. Liu, H., Dilger,JP. & Lin, J. A pan-cancer-bioinformatic-based literature review of TRPM7 in cancers. *Front Oncol*. **12**,858756. https://doi.org/10.3389/fonc.2022.858756 (2022).
45. Liu, H., Weng, J., Huang, C. L., & Jackson, A. P. Voltage-gated sodium channels in cancers. *Biomark Res.* **12**, 70. https://doi.org/10.1186/s40364-024-00620-x (2024).
46. Liu, H., & Tang, T. Pan-cancer genetic analysis of cuproptosis and copper metabolism-related gene set. *Front Oncol*. **12**, 952290. https://doi.org/10.3389/fonc.2022.952290 (2022).
47. Pan, Y. C., Nishikawa, T., Chang, C. Y., Tai, J. A., & Kaneda, Y. CXCL2 combined with HVJ-E suppresses tumor growth and lung metastasis in breast cancer and enhances anti-PD-1 antibody therapy. *Mol Ther Oncolytics*. **20**, 175-186. https://doi.org/10.1016/j.omto.2020.12.011 (2022).
48. Yu, X. et al. SHCBP1 Promotes the Proliferation of Breast Cancer Cells by Inhibiting CXCL2. *J Cancer*. **14**, 3444-3456. https://doi.org/10.7150/jca.88072 (2023).
49. You, J. et al. TNFSF15 and MIA Variant Associated with Immunotherapy and Prognostic Evaluation in Esophageal Cancer. *Journal of Oncology* 1–12, (2023). https://doi.org/10.1155/2023/1248024 (2023).
50. Lu, J., Hu, F., Zhou, Y. & Guo, X. NR3C2-Related transcriptome profile and clinical outcome in invasive breast carcinoma. *Biomed. Res. Int.* **2021**, 1–13. https://doi.org/10.1155/2021/9025481 (2021).
51. Fan, Y. et al. miR-301b-3p regulates breast Cancer cell proliferation, migration, and invasion by targeting NR3C2. *J. Oncol.* **2021**, 1–9. https://doi.org/10.1155/2021/8810517 (2021).
52. Giacomini, A., Ghedini, G. C., Presta, M. & Ronca, R. Long pentraxin 3: A novel multifaceted player in cancer. *Biochim. Et Biophys. Acta (BBA) - Reviews Cancer*. **1869**, 53–63. https://doi.org/10.1016/j.bbcan.2017.11.004 (2018).
53. Giacomini, A. et al. The PTX3/TLR4 autocrine loop as a novel therapeutic target in triple negative breast cancer. *Experimental Hematol. Oncol.* **12** https://doi.org/10.1186/s40164-023-00441-y (2023).
54. Wu, J., Yang, R., Ge, H., Zhu, Y. & Liu, S. PTX3 promotes breast cancer cell proliferation and metastasis by regulating PKCζbreast cancer, pentraxin 3, protein kinase Cζ, proliferation, metastasis. *Experimental Therapeutic Med.* **27** https://doi.org/10.3892/etm.2024.12412 (2024).
55. Yen, M. C. et al. S100B expression in breast cancer as a predictive marker for cancer metastasis. *Int. J. Oncol.* https://doi.org/10.3892/ijo.2017.4226 (2017).
56. Rybinska, I. et al. SAA1-dependent reprogramming of adipocytes by tumor cells is associated with triple negative breast cancer aggressiveness. *Int. J. Cancer*. **154**, 1842–1856. https://doi.org/10.1002/ijc.34859 (2024).
57. Malle, E. & De Beer, F. C. Human serum amyloid A (SAA) protein: a prominent acute-phase reactant for clinical practice. *Eur. J. Clin. Invest.* **26**, 427–435. https://doi.org/10.1046/j.1365-2362.1996.159291.x (2003).
58. Razis, E. et al. The role of CXCL13 and CXCL9 in early breast Cancer. *Clin. Breast. Cancer.* **20**, e36–e53. https://doi.org/10.1016/j.clbc.2019.08.008 (2020).

Author contributions

HJ contributed to the notion of this research. TD designed the research strategy and completed the first manuscript. YC revised the manuscript. LL and YZ performed IHC and data analysis. WP, JL, YL, and YW helped perform the analysis with constructive discussions. All authors contributed to the article and approved the submitted manuscript.

Funding
The research fund was provided by Research Project Supported by Shanxi Scholarship Council of China (2021 – 157), Open Fund from Key Laboratory of Cellular Physiology (CPOF202310), Wu Jieping Medical Fund (320.6750.2023-18-121), Shanxi natural Science Project youth project (202303021222339), The central government leads the local science and technology development fund project (YDZJSX2024D068), China Postdoctoral Science Foundation (2021M691993), Doctoral Research Project of Shanxi Medical University (XD1901), Postgraduate Practice Innovation Project in Shanxi Province (2024SJ166).

Declarations

Competing interests
The authors declare no competing interests.

Ethics declarations
This research was conducted according to the guidelines of the Declaration of Helsinki, and approved by the Ethics Committee at the First Hospital of Shanxi Medical University (Approval ID: NO.KYLL-2024-034).

Consent to publish
All authors gave consent for publication.

Additional information
Supplementary Information The online version contains supplementary material available at https://doi.org/10.1038/s41598-025-00891-w.

Correspondence and requests for materials should be addressed to Y.C., Y.W. or H.J.

Reprints and permissions information is available at www.nature.com/reprints.

Publisher's note Springer Nature remains neutral with regard to jurisdictional claims in published maps and institutional affiliations.